International Journal of Applied Mathematics and Theoretical Physics
2026, Vol. 12, No. 3, pp. 94–105
https://doi.org/10.11648/j.ijamtp.20261203.12

Research Article

Unsteady Magnetohydrodynamic Flow of a Chemically Reactive Fluid Past an Inclined Porous Plate Embedded in a Porous Medium with Thermal-Diffusion Effects

Henry Martyns, Liberty Ebiwareme*, Roseline Ize Ndu

Department of Mathematics, Rivers State University, Port Harcourt, Nigeria

Abstract

This study elucidates the unsteady magnetohydrodynamic (MHD) flow of a chemically reactive, electrically conducting fluid past an inclined porous plate embedded in a saturated porous medium, considering the effects of chemical reaction and thermal diffusion. The governing equations describing momentum, energy, and species transport are formulated under the boundary-layer approximation, accounting for magnetic field, porous medium resistance, thermal and solutal buoyancy, plate inclination, and flow unsteadiness. The dimensionless governing equations are solved via the regular perturbation method, and the effects of the controlling parameters on the velocity, temperature, and concentration fields are examined alongside the skin-friction coefficient, local Nusselt number, and Sherwood number. The results show that increasing the magnetic field strength and porous medium resistance suppresses fluid motion, whereas thermal and solutal buoyancy enhance the flow. Soret effect promotes species diffusion by enhancing mass transfer induced by temperature gradients. In contrast, stronger chemical reactions reduce concentration levels within the boundary layer. The interaction of these physical mechanisms significantly influences the momentum, heat, and mass transfer characteristics. The findings offer valuable theoretical insights for analyzing and optimizing reactive MHD transport processes in porous media, with applications in chemical processing, thermal engineering, and energy conversion systems.

Keywords

Thermal-diffusion, Chemical Reaction, Viscous Dissipation, Porous Medium, MHD

1. Introduction

Magnetohydrodynamics (MHD) concerns the motion of electrically conducting fluids under the influence of magnetic fields, where the interaction between the fluid and the applied magnetic field generates Lorentz forces that significantly alter the velocity, temperature, and concentration fields. Owing to its ability to control and manipulate electrically conducting fluids, MHD has attracted considerable research attention because of its wide range of applications in engineering and industrial processes, including nuclear reactor cooling, plasma confinement, electromagnetic pumping, metallurgical processing, and liquid-metal technologies [1, 2]. These applications have motivated extensive investigations into MHD transport phenomena under different thermal, hydrodynamic,

*Correspondence: Liberty Ebiwareme (liberty.ebiwareme@ust.edu.ng)

Received: 10 August 2026; **Accepted:** 22 August 2026; **Published:** 15 September 2026

and mass-transfer conditions. Unsteady MHD flows are particularly important because they describe transient transport phenomena that cannot be adequately captured by steady-state analyses. In practical engineering systems, temporal variations in flow conditions, heat transfer, species diffusion, and chemical reactions frequently occur, making the investigation of unsteady MHD transport essential for accurately predicting the behavior of electrically conducting fluids under realistic operating conditions [3, 4].

Porous media constitute another important aspect of many engineering and environmental systems because they introduce resistance to fluid motion and thereby modify momentum, heat, and mass transport characteristics. Applications involving geothermal reservoirs, packed-bed reactors, filtration systems, petroleum recovery, heat exchangers, and thermal insulation frequently involve fluid flow through porous structures [5]. The complexity of such flows is further increased when transport occurs over inclined surfaces, since the inclination changes the gravitational component acting along the plate and consequently alters the buoyancy-driven flow structure. The simultaneous presence of porous resistance, buoyancy forces, and externally applied magnetic fields therefore provides a more realistic representation of numerous industrial transport processes than conventional vertical-plate configurations. Previous studies have demonstrated that plate inclination and porous media substantially influence velocity, thermal boundary-layer development, flow stability, and convective heat and mass transfer characteristics [6].

In many industrial applications, fluid motion is accompanied by chemical reactions and internal heat generation or absorption, both of which considerably influence thermal and concentration distributions within the boundary layer. Examples include combustion systems, catalytic reactors, chemical processing equipment, environmental pollutant transport, and energy conversion devices, where reactive species interact continuously with thermal fields [7]. Furthermore, cross-diffusion mechanisms such as the Soret (thermal-diffusion) and Dufour (diffusion-thermo) effects establish additional coupling between heat and mass transfer, thereby increasing the complexity of the transport process [8]. These interacting mechanisms become even more significant in transient MHD flows through porous media, where neglecting any of the coupled physical effects may result in inaccurate prediction of engineering quantities such as skin friction, heat transfer rate, and mass transfer rate. Consequently, comprehensive mathematical models capable of simultaneously accounting for these phenomena are indispensable for the design and optimization of modern thermal engineering systems.

Extensive investigations have therefore been devoted to MHD free-convective transport over porous surfaces using different mathematical models and numerical approaches. An investigation of unsteady MHD free-convective heat and mass transfer through a porous medium was conducted using the regular perturbation method [9]. Their findings showed that the magnetic field, permeability, heat source, chemical reaction, and buoyancy forces significantly influence the velocity, temperature, and concentration fields as well as the skin-friction coefficient, Nusselt number, and Sherwood number. Subsequently, [10] employed the finite element method to study unsteady MHD free convection of polar fluids with heat generation and thermal diffusion, while [11] incorporated Hall current, thermal radiation, variable temperature, and thermal diffusion into the analysis of transient MHD flow over an inclined plate. The finite difference technique was adopted by [12] to investigate MHD flow over a semi-infinite inclined plate, whereas [13] incorporated velocity slip, chemical reaction, and thermodiffusion effects. More recently, [14-16] extended these analyses by including porous media, radiation absorption, diffusion-thermo effects, chemical reactions, and non-Newtonian fluid behavior. Likewise, [17] employed computational fluid dynamics to investigate Jeffrey fluid flow over an inclined porous plate. Collectively, these studies demonstrate a progressive advancement in MHD transport analysis through increasingly realistic physical models and robust numerical techniques.

Apart from numerical investigations, considerable progress has also been achieved through semi-analytical and analytical solution techniques. The Adomian decomposition method was successfully applied by [18] to investigate MHD flow past an infinite vertical porous plate, demonstrating the significant influence of magnetic field strength, suction, permeability, thermal radiation, Eckert number, Grashof number, Prandtl number, and porosity on the flow and heat transfer characteristics. Subsequently, [19] extended the ADM to Casson fluid flow over an inclined porous plate with radiation absorption and chemical reaction. Furthermore, [20] employed the Temimi-Ansari Method (TAM), [21] utilized the Reduced Differential Transformation Method (RDTM) to obtain accurate semi-analytical solutions for related MHD transport problems. These investigations demonstrated that analytical approximation techniques provide accurate and computationally efficient solutions while offering deeper physical insight into the influence of governing parameters on velocity, temperature, and concentration distributions.

Despite these remarkable advances, important gaps still exist in the available literature. Most previous investigations have examined magnetic field effects, porous medium resistance, chemical reactions, thermal radiation, viscous dissipation, heat generation or absorption, and cross-diffusion phenomena either independently or in limited combinations. Consequently, relatively few studies have developed a unified mathematical framework that simultaneously incorporates flow unsteadiness, porous medium resistance, thermal radiation, viscous dissipation, heat generation or absorption, first-order chemical reaction, Soret effect, Dufour effect, and plate inclination. Moreover, many existing studies rely primarily on numerical techniques, which, although highly accurate, often provide limited analytical insight into the physical mechanisms governing transport processes. These limitations underscore the need for a more comprehensive analytical model capable of accurately describing transient MHD transport under realistic engineering conditions.

The present study addresses this research gap by developing a comprehensive mathematical model for the unsteady two-dimensional flow of an incompressible, viscous, electrically conducting, chemically reactive fluid past an infinite inclined porous plate embedded in a homogeneous saturated porous medium. The model simultaneously incorporates thermal radiation, viscous dissipation, heat generation (or absorption), thermal-diffusion (Soret effect), diffusion-thermo (Dufour effect), and first-order homogeneous chemical reaction under the influence of a transverse magnetic field. The governing dimensional equations are transformed into their corresponding dimensionless forms and solved analytically using the regular perturbation method. The effects of the governing dimensionless parameters—including the magnetic field parameter, porosity parameter, thermal and solutal Grashof numbers, Prandtl number, Schmidt number, heat generation parameter, thermal radiation parameter, Soret parameter, Dufour number, chemical reaction parameter, and angle of inclination—on the velocity, temperature, and concentration distributions are thoroughly examined together with the engineering quantities of practical interest, namely the skin-friction coefficient, local Nusselt number, and local Sherwood number. The novelty of this study lies in integrating these strongly coupled transport mechanisms within a unified analytical framework while providing approximate closed-form solutions that facilitate clearer physical interpretation of the governing transport processes.

Beyond its methodological contribution, this study provides valuable theoretical and engineering insights into the combined effects of magnetic field strength, porous medium permeability, thermal and solutal buoyancy, heat generation or absorption, thermal radiation, chemical reaction, Soret and Dufour effects on transient transport phenomena in electrically conducting fluids. The findings are expected to contribute to the improved design and optimization of engineering systems involving geothermal energy extraction, chemical reactors, thermal management devices, filtration technologies, metallurgical operations, and other industrial processes involving coupled heat and mass transfer in porous media. The remainder of this paper is organized as follows. Section 2 presents the mathematical formulation of physical problems together with the governing equations and boundary conditions. Section 3 describes the nondimensionalization procedure, while Section 4 presents the regular perturbation solution methodology. Section 5 defines the engineering quantities of interest, followed by the discussion of numerical results in Section 6. Finally, Section 7 summarizes the principal findings, conclusions, and engineering implications of the present investigation.

2. Mathematical Formulation of the Problem

Consider the unsteady, two-dimensional, laminar, incompressible, electrically conducting fluid flow of a chemically reactive fluid past an infinite inclined porous plate embedded in a homogeneous porous medium. The plate is inclined at an angle to the vertical. A uniform magnetic field of strength is imposed perpendicular to the plate. The induced magnetic field is neglected because the magnetic Reynolds number is assumed to be sufficiently small. The fluid properties are considered constant except for density variations in the buoyancy terms, which are incorporated using the Boussinesq approximation. The coordinate system is chosen such that the axis is along the plate, while the other axis is normal to it. A constant suction velocity is imposed at the wall. Heat transfer is influenced by thermal radiation, viscous dissipation, heat generation (or absorption), and the Dufour effect, while mass transfer is affected by thermal diffusion and a first-order homogeneous chemical reaction. Under these assumptions, the governing equations are provided as follows.

Continuity Equation

$$\frac{\partial \grave{u}}{\partial x} + \frac{\partial \grave{\bar{v}}}{\partial y}$$

Given that the vertical suction/injection $v = -v_0$ (constant), the continuity equation reduces to

$$\frac{\partial \bar{v}}{\partial y} = 0 \Longrightarrow \bar{v} = -v_0 \text{ (constant)} \tag{1}$$

Momentum Equation (x-direction)

$$\frac{\partial \bar{u}}{\partial \bar{y}} + \bar{v}\frac{\partial \bar{u}}{\partial \bar{y}} = \lambda \frac{\partial^2 \bar{u}}{\partial \bar{y}^2} + g\beta_c(\bar{C} - \bar{C}_\infty)\cos\alpha + g\beta_T(\bar{T} - \bar{T}_\infty)\cos\alpha - \frac{\sigma B_0^2}{\rho}\bar{u} - \frac{\lambda \bar{u}}{\bar{k}} \tag{2}$$

Energy Equation

$$\rho C_p\left(\frac{\partial \bar{T}}{\partial \bar{t}} + \bar{v}\frac{\partial \bar{T}}{\partial \bar{y}}\right) = k\frac{\partial^2 \bar{T}}{\partial \bar{y}^2} + \mu\left(\frac{\partial \bar{u}}{\partial \bar{y}}\right)^2 -$$

$$\frac{\partial q_r}{\partial \bar{y}} + \frac{\rho D_m k_T}{C_s}\frac{\partial^2 \bar{C}}{\partial \bar{y}^2} - Q_0(\bar{T} - \bar{T}_\infty) \tag{3}$$

Concentration Equation

$$\frac{\partial \bar{C}}{\partial \bar{t}} + \bar{v}\frac{\partial \bar{C}}{\partial \bar{y}} = D\frac{\partial^2 \bar{C}}{\partial \bar{y}^2} + \frac{D_m k_T}{T_m}\frac{\partial^2 \bar{T}}{\partial \bar{y}^2} - k_r(\bar{C} - \bar{C}_\infty) \tag{4}$$

The appropriate boundary and initial conditions are given as follows:

$$\bar{t} \le 0, \bar{u} = 0, \bar{T} = \bar{T}_\infty, \bar{C} = \bar{C}_\infty \text{ for all } y$$

$$\bar{t} > 0, \bar{u} = u_0, \bar{v} = -v_0, \bar{T} = \bar{T} + (\bar{T}_w - \bar{T}_\infty)e^{A\bar{t}}, \bar{C} = \bar{C} + (\bar{C}_w - \bar{C}_\infty)e^{A\bar{t}} \text{ at } \bar{y} = 0 \tag{5}$$

$$\bar{u} = 0, \bar{T} \to \infty, \bar{C} \to \infty, \bar{y} \to \infty$$

where $A = \frac{v_0^2}{\lambda}$ denotes the unsteadiness parameter. The symbols $(\grave{u}, \grave{v})$ represent the velocity components in the x- and y-directions, respectively, and t denotes time. The parameter λ corresponds to the kinematic viscosity of the fluid, while g is the gravitational acceleration. The coefficients β_T and β_C represent the thermal and solutal expansion coefficients, respectively. $\grave{T}$and $\grave{C}$are the local fluid temperature and concentration, whereas $\grave{T}_\infty$ and $\grave{C}_\infty$ denote the ambient temperature and concentration. The inclination of the plate is given by α. The electrical conductivity of the fluid is represented by σ, and B_0 denotes the applied magnetic field intensity. The fluid density is ρ, and the permeability of the porous medium is k. Thermal properties include the specific heat at constant pressure C_p and the thermal conductivity k, while μ represents dynamic viscosity. Radiative heat flux is denoted by $\grave{q}_r$. Molecular diffusion is characterized by D_m, and k_T represents the thermal diffusion (Soret) coefficient. C_s is the reference concentration scaling constant, and Q_0 denotes the heat generation or absorption coefficient. Mass diffusion is represented by D, and T_m is the reference temperature for the Soret effect. The chemical reaction rate is given by k_r. The wall temperature and concentration are denoted by T_w and C_w, respectively. Finally, u_0 is the characteristic plate velocity, and v_0 corresponds to the wall suction or blowing velocity.

3. Nondimensionalization and Reduction to ODEs

To reduce the radiative heat flux in the temperature equation, we use the Rosseland approximation for a thick fluid, wherein we express the radiative heat flux term as

$$q_r = -\frac{4\sigma}{3\bar{k}}\frac{\partial \bar{T}^4}{\partial \bar{y}} \tag{6}$$

Here σ and $\bar{k}$ represents the Stefan-Boltzmann constant and mean absorption. Supposing small temperature differences within the fluid, then we express $\bar{T}^4$ as a linear function of the temperatures. Expanding on $\bar{T}_\infty$ using Taylor's series and ignoring higher-order terms, we obtain the form

$$\bar{T}^4 \approx 4\bar{T}_\infty^3 - 3T_\infty^4 \tag{7}$$

Putting Eqs. (6) and (7), the reduced form of Eq. (3) is given as

$$\rho C_p\left(\frac{\partial \bar{T}}{\partial \bar{t}} + \bar{v}\frac{\partial \bar{T}}{\partial \bar{y}}\right) = k\frac{\partial^2 \bar{T}}{\partial \bar{y}^2} + \frac{16\sigma \bar{T}_\infty^3}{3\bar{k}}\frac{\partial^2 \bar{T}}{\partial \bar{y}^2} + \frac{\rho D_m k_T}{C_s}\frac{\partial^2 \bar{C}}{\partial \bar{y}^2} + -Q_0(\bar{T} - \bar{T}_\infty) \tag{8}$$

To make the governing equations dimensionless, we choose the following dimensional quantities as

$$u = \frac{\bar{u}}{u_0}, t = \frac{\bar{t}v_0^2}{\lambda}, \theta = \frac{\bar{T} - \bar{T}_\infty}{\bar{T}_w - \bar{T}_\infty}, \phi = \frac{\bar{C} - \bar{C}_\infty}{\bar{C}_w - \bar{C}_\infty}, Gc = \frac{\lambda\beta_C(\bar{C}_w - \bar{C}_\infty)}{u_0 v_0^2}, Gr = \frac{\lambda\beta_T(\bar{T}_w - \bar{T}_\infty)}{u_0 v_0^2}$$

$$Du = \frac{D_m k_T(\bar{C}_w - \bar{C}_\infty)}{C_s C_p \lambda(\bar{T}_w - \bar{T}_\infty)}, Sr = \frac{D_m k_T(\bar{T}_w - \bar{T}_\infty)}{T_m \lambda(\bar{C}_w - \bar{C}_\infty)}, \kappa = \frac{v_0^2 \bar{k}}{\lambda^2}, Pr = \frac{\mu C_p}{k}, M^2 = \frac{\sigma B_0^2 \lambda}{\rho v_0^2}, R = \frac{4\sigma \bar{T}_\infty^3}{k\bar{k}}$$

$$Kr = \frac{k_r \lambda}{v_0^2}, Q = \frac{Q_0 \lambda}{\rho C_p v_0^2}, Sc = \frac{\lambda}{D_m}, y = \frac{\bar{y} v_0}{\lambda} \tag{9}$$

The governing equations (2), (3), and (8) in non-dimensional form, using Eq. (9), yield the form

$$\frac{\partial u}{\partial t} - \frac{\partial u}{\partial y} = \frac{\partial^2 u}{\partial y^2} + (Gr\theta + Gc\phi)\cos\alpha - \left(M^2 + \frac{1}{K}\right)u \tag{10}$$

$$\frac{\partial \theta}{\partial t} - \frac{\partial \theta}{\partial y} = \frac{1}{Pr}\left(1 + \frac{4R}{3}\right)\frac{\partial^2 \theta}{\partial y^2} + Du\frac{\partial^2 \phi}{\partial y^2} - Q\theta \tag{11}$$

$$\frac{\partial \phi}{\partial t} - \frac{\partial \phi}{\partial y} = \frac{1}{Sc}\frac{\partial^2 \phi}{\partial y^2} + Sr\frac{\partial^2 \theta}{\partial y^2} - Kr\phi \tag{12}$$

The initial and boundary conditions in dimensionless form are given as

$$t \le 0, u = 0, \theta = 0, \phi = 0 \text{ for all } y$$

$$t > 0, u = 1, \theta = e^t, \phi = e^t \text{ at } y = 0 \tag{13}$$

$$u = 0, u \to 0, y \to 0$$

4. Solution of the Problem

The coupled dimensionless governing Eqs. (10) - (12), together with the boundary conditions (13), constitute a system of linear partial differential equations describing the transient momentum, heat, and mass transfer within the boundary layer.

Since the wall velocity, temperature, and concentration are assumed to experience small periodic disturbances of amplitude ε, where $0 < \varepsilon \ll 1$, the regular perturbation method provides an efficient analytical technique for obtaining approximate closed-form solutions. The method consists of expanding the dependent variables as asymptotic series in terms of the perturbation parameter and solving the resulting hierarchy of boundary-value problems successively.

We assume the following perturbation expansions of the form

$$u(y,t) = u_0(y) + \varepsilon e^{nt} u_1(y) + O(\varepsilon^2) \tag{14}$$

$$\theta(y,t) = \theta_0(y) + \varepsilon e^{nt} \theta_1(y) + O(\varepsilon^2) \tag{15}$$

$$\phi(y,t) = \phi_0(y) + \varepsilon e^{nt} \phi_1(y) + O(\varepsilon^2) \tag{16}$$

where u_0, θ_0, ϕ_0 denote the steady (zeroth-order) solutions, while u_1, θ_1, ϕ_1 represent the first-order corrections resulting from the imposed temporal disturbance. Substituting Eqs. (14)-(16) into the governing Eqs. (10) - (12), expanding the resulting expressions, and collecting coefficients of equal powers of ε produce two independent systems of ordinary differential equations corresponding to the zeroth and first perturbation orders.

$$u_0'' + Su_0' - (M+K)u_0 = -Gr\,\theta_0 \cos\alpha - Gc\,\phi_0 \cos\alpha \tag{17}$$

$$\frac{1+R}{Pr}\theta_0'' + S\theta_0' + Q\theta_0 = 0 \tag{18}$$

$$\frac{1}{Sc}\phi_0'' + S\phi_0' - \mathrm{Kr}\phi_0 = -Sr\,\theta_0'' \tag{19}$$

subject to the boundary condition

$$u_0(0) = 1, \theta_0(0) = 1, \phi_0(0) = 1$$

$$u_0(\infty) = 0, \theta_0(\infty) = 0, \phi_0(\infty) = 0 \tag{20}$$

Eq. (18) is a linear second-order differential equation with constant coefficients. We seek a solution of exponential form

$$\theta_0 = e^{-m_1 y} \tag{21}$$

substitution into Eq. (18) gives the characteristic equation become

$$\frac{1+R}{Pr}m_1^2 - Sm_1 + Q = 0 \tag{22}$$

Similarly,

$$\theta_0(\eta) = e^{-m_1 y} \tag{23}$$

Upon substitution, Eq. (19) reduced to the form

$$\frac{1}{Sc}\phi_0'' + S\phi_0' - K_r\phi_0 = -Sr\,m_1^2 e^{-m_1 y} \tag{24}$$

The complementary solution of Eq. (24) satisfies

$$\frac{1}{Sc}m^2 - Sm - K_r = 0 \tag{25}$$

The non-homogeneous term possesses the same exponential dependence as the temperature field. Therefore, a particular solution is assumed in the form

$$\phi_{0p} = Ae^{-m_1 y} \tag{26}$$

Substituting Eq. (26) into Eq. (25) gives the value of the constant A ad consequently

$$\phi_0(y) = C_1 e^{-m_2 y} + Ae^{-m_1 y} \tag{27}$$

Applying the wall boundary condition, $\phi_0(0) = 1$ yields the constant

$$\phi_0(y) = (1-A)e^{-m_2 y} + Ae^{-m_1 y} \tag{28}$$

In view of the above, the momentum equation may now be solved as follows

$$u_0'' + Sv_0' - (M+K)u_0 = -Gr\cos\alpha\, e^{-m_1 y} - Gc\cos\alpha[(1-A)e^{-m_2 y} + Ae^{-m_1 y}] \tag{29}$$

The complementary solution satisfies

$$m^2 - Sm - (M+K) = 0 \tag{30}$$

Motivated by the forcing terms appearing on the right-hand side of Eq. (33), the particular solution is assumed as

$$u_{0p} = Be^{-m_1 y} + Ce^{-m_2 y} \tag{31}$$

Accordingly, the complete zeroth-order velocity distribution becomes

$$u_0(y) = C_2 e^{-m_3 y} + Be^{-m_1 y} + Ce^{-m_2 y} \tag{32}$$

Finally, imposing the wall condition, $u_0(0) = 1$, the constant is found and Eq. (32) is reduced to

$$u_0(y) = (1-B-C)e^{-m_3 y} + Be^{-m_1 y} + Ce^{-m_2 y} \tag{33}$$

First-Order Problem

$$u_1'' + Su_1' - (M + K + n)u_1 = -Gr\theta_1 \cos\alpha - Gc\phi_1 \cos\alpha \tag{34}$$

$$\frac{1+R}{Pr}\theta_1'' + S\theta_1' + (Q - n)\theta_1 = 0 \tag{35}$$

$$\frac{1}{Sc}\phi_1'' + S\phi_1' - (K_r + n)\phi_1 = -Sr\theta_1'' \tag{36}$$

subject to the appropriate boundary conditions

$$\left.\begin{array}{c} u_1(0) = 1, \theta_1(0) = 1, \phi_1(0) = 1 \\ u_1(\infty) = 0, \theta_1(\infty) = 0, \phi_1(\infty) = 0 \end{array}\right\} \tag{37}$$

The energy equation (35) is first considered. Since it possesses constant coefficients, an exponentially decaying solution is assumed in the form

$$\theta_1 = e^{-m_4 y} \tag{38}$$

Substituting Eq. (38) into Eq. (36) yields the characteristic equation

$$\frac{1+R}{Pr}m_4^2 - Sm_4 + (Q - n) = 0 \tag{39}$$

Substituting Eq. (38) into Eq. (44) reduces to the form

$$\frac{1}{Sc}\phi_1'' + S\phi_1' - (\mathrm{Kr} + n)\phi_1 = -Sr\, m_4^2 e^{-m_4 y} \tag{40}$$

The corresponding complementary equation possesses the characteristic equation

$$\frac{1}{Sc}m^2 - Sm - (K_r + n) = 0 \tag{41}$$

The forcing term in Eq. (40) suggests the particular solution

$$\phi_{1p} = De^{-m_4 y} \tag{42}$$

$$\phi_1(\eta) = D_1 e^{-m_5 y} + De^{-m_4 y} \tag{43}$$

Applying the boundary condition, $\phi_1(0) = 1$, and consequently Eq. (43) takes the form

$$\phi_1(\eta) = (1 - D)e^{-m_5 y} + De^{-m_4 y} \tag{44}$$

The concentration solution obtained above is substituted into the momentum Eq. (34). Thus,

$$u_1'' + Su_1' - (M + K + n)u_1 = -Gr\cos\alpha\, e^{-m_4 y} - Gc\cos\alpha[(1 - D)e^{-m_5 y} + De^{-m_4 y}] \tag{45}$$

The corresponding homogeneous equation possesses the characteristic equation

$$m^2 - Sm - (M + K + n) = 0 \tag{46}$$

Motivated by the non-homogeneous terms appearing in Eq. (58), the particular solution is assumed in the form

$$u_{1p} = Ee^{-m_4 y} + Fe^{-m_5 y} \tag{47}$$

Substitution into Eq. (45) yields the required constants, hence the first approximation for the velocity becomes

$$u_1(y) = E_1 e^{-m_6 y} + Ee^{-m_4 y} + Fe^{-m_5 y} \tag{48}$$

Inserting the boundary condition, $u_1(0) = 1$, yield the expression

$$u_1(\eta) = (1 - E - F)e^{-m_6 \eta} + Ee^{-m_4 \eta} + Fe^{-m_5 \eta} \tag{49}$$

The complete analytical first-order solutions obtained above represent the transient response of the velocity, temperature, and concentration fields to the imposed periodic disturbance at the wall.

$$u(y,t) = (1 - B - C)e^{-m_3 y} + Be^{-m_1 y} + Ce^{-m_2 y} + \varepsilon e^{nt}[(1 - E - F)e^{-m_6 y} + Ee^{-m_4 y} + Fe^{-m_5 y}] \tag{50}$$

$$\theta(y,t) = e^{-m_1 y} + \varepsilon e^{nt} e^{-m_4 y} \tag{51}$$

$$\phi(y,t) = (1 - A)e^{-m_2 y} + Ae^{-m_1 y} + +\varepsilon e^{nt}[(1 - D)e^{-m_5 y} + De^{-m_4 y}] \tag{52}$$

5. Engineering Quantities

An important set of engineering quantities associated with momentum, heat, and mass transport is the skin-friction coefficient, the Nusselt number, and the Sherwood number, respectively. These parameters quantify the wall shear stress, the dimensionless rate of heat transfer, and the dimensionless rate of mass transfer at the plate surface. They provide valuable insight into the transport characteristics of the flow and the influence of the governing physical parameters. In dimensionless form, they are defined as follows:

$$C_f = -\left(\frac{\partial u}{\partial y}\right)_{y=0} = m_3(1 - B - C) + m_1 B + m_2 C + \varepsilon e^{nt}[m_6(1 - E - F) + m_4 E + m_5 F] \tag{53}$$

$$Nu_x = -\left(\frac{\partial \theta}{\partial y}\right)_{y=0} = m_1 + \varepsilon e^{nt} m_4 \tag{54}$$

$$Sh_x = -\left(\frac{\partial \phi}{\partial y}\right)_{y=0} = m_2(1 - A) + m_1 A + +\varepsilon e^{nt}[m_5(1 - D) + m_4 D] \tag{55}$$

6. Results and Discussion

The effects of the governing dimensionless parameters on the velocity, temperature, and concentration profiles are presented in Figures 1-15. These results illustrate the influence of the controlling physical parameters on the momentum, thermal, and concentration boundary layers. To clearly identify the role of each parameter, a one-parameter-at-a-time analysis was performed, whereby a single dimensionless parameter was varied while all other parameters were maintained at their baseline values. This approach enables the individual contribution of each parameter to the transport characteristics of the flow to be isolated and interpreted based on the underlying mechanisms governing momentum, heat, and mass transfer. Unless otherwise stated, numerical computations were carried out using the following reference values of the governing dimensionless parameters: $M = 1.0, K = 0.5, Gr = 2.0, Gc = 2.0, Pr = 0.71, R = 0.50, Q = 0.20, Sc = 0.62, Sr = 0.40, Kr = 0.50, n = 0.20, \alpha = 30^0, S = 4, \varepsilon = 0.02, t = 1$. Throughout the parametric study, only the parameters of interest was varied, while the remaining parameters were held fixed at these reference values to facilitate a systematic assessment of their individual effects on the velocity, temperature, and concentration fields.

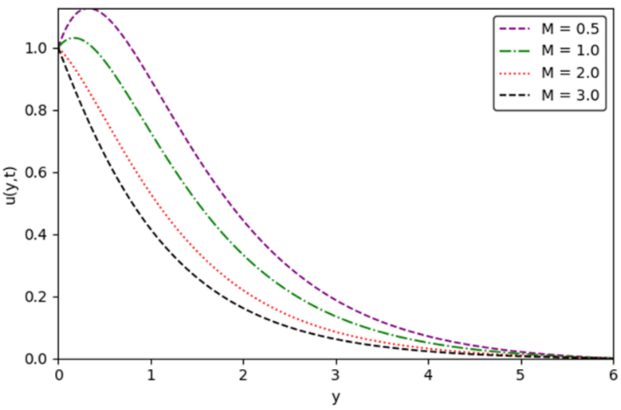

Figure 1. *Effect of Magnetic field parameter on the velocity profile.*

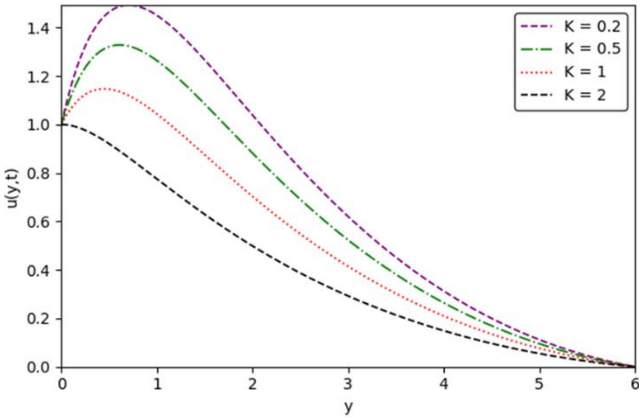

Figure 2. *Influence of porosity parameter on the velocity profile.*

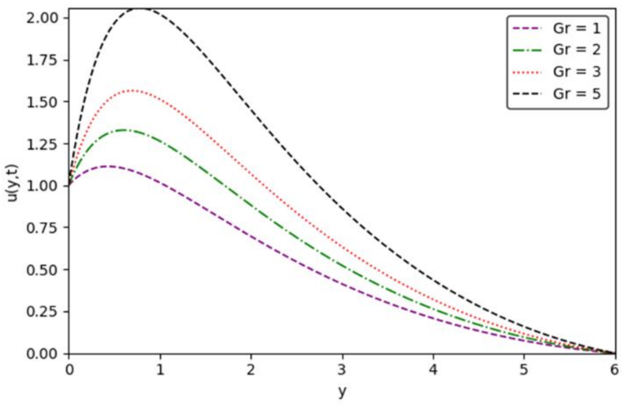

Figure 3. *Variation of thermal Grashof number with velocity profile.*

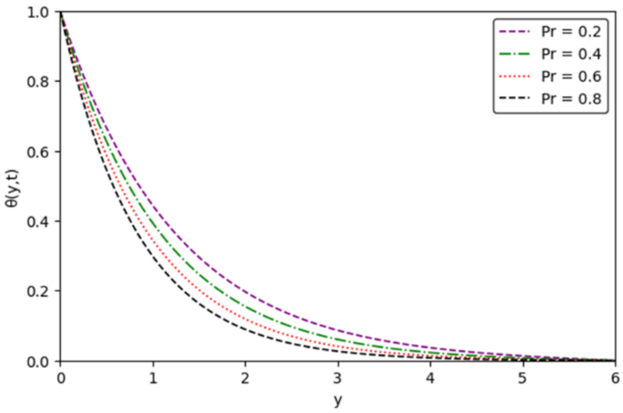

Figure 4. *Effect of Prandtl number on the temperature profile.*

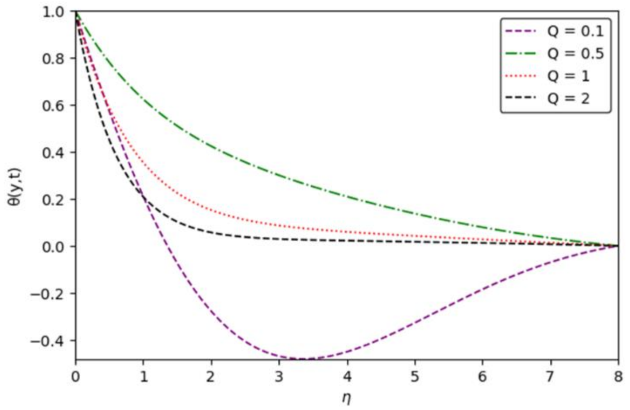

Figure 5. Effect of heat generation parameter on temperature profile.

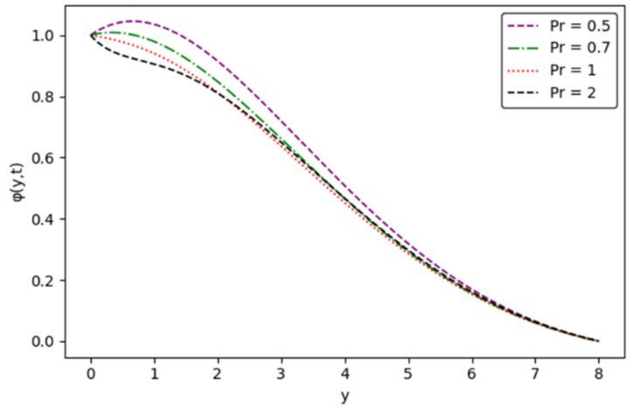

Figure 8. Effect of Prandtl number on concentration profile.

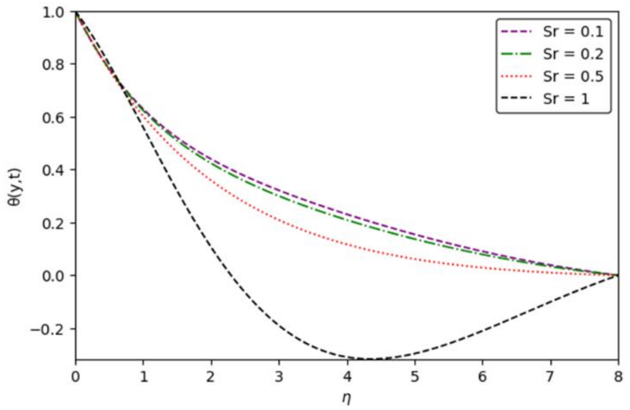

Figure 6. Effect of Soret parameter on the temperature profile.

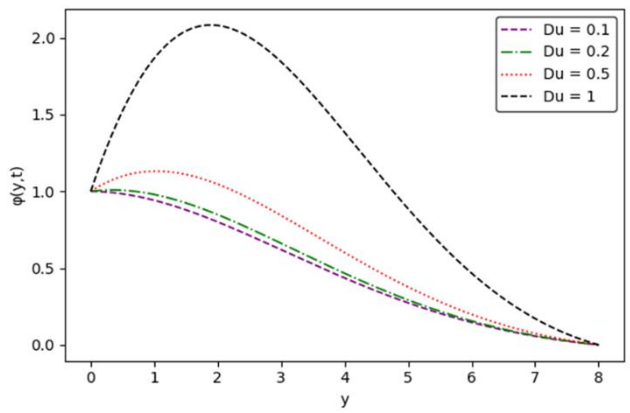

Figure 9. Influence of DuFour parameter on the concentration profile.

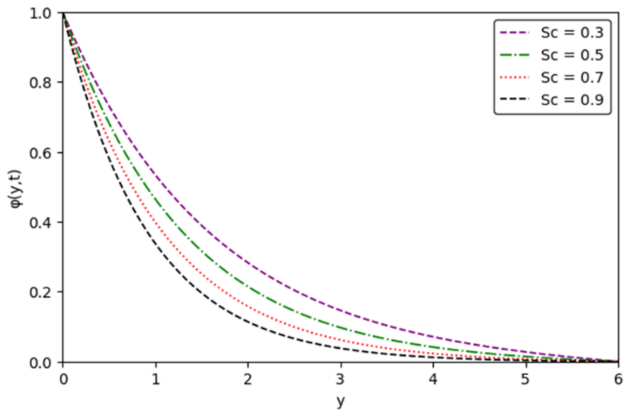

Figure 7. Effect of Schmidt number on the concentration profile.

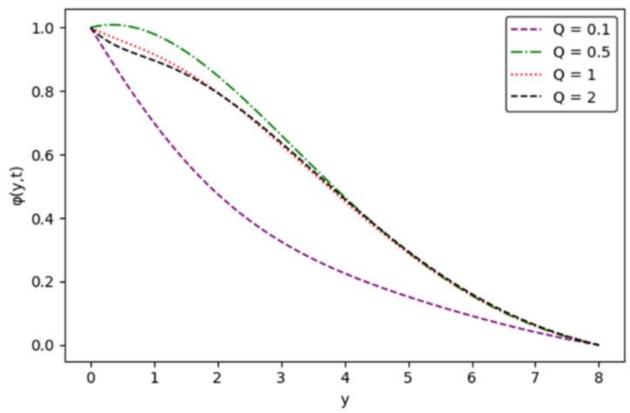

Figure 10. Influence of heat generation parameter on concentration profile.

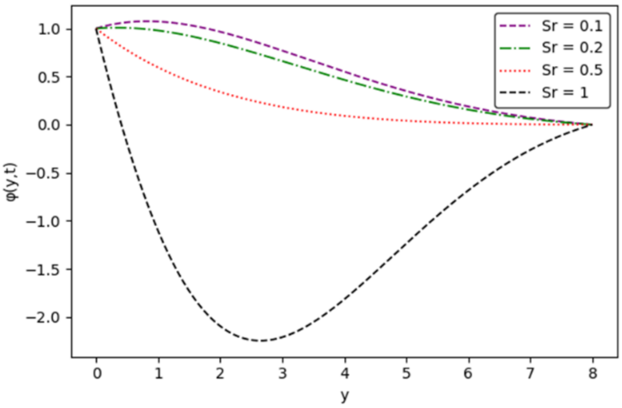

Figure 11. *Effect of Soret parameter on the concentration profile.*

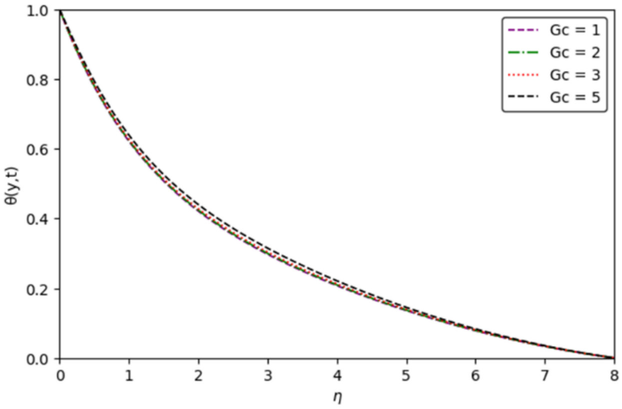

Figure 12. *Influence of Mass Grashof number on the temperature profile.*

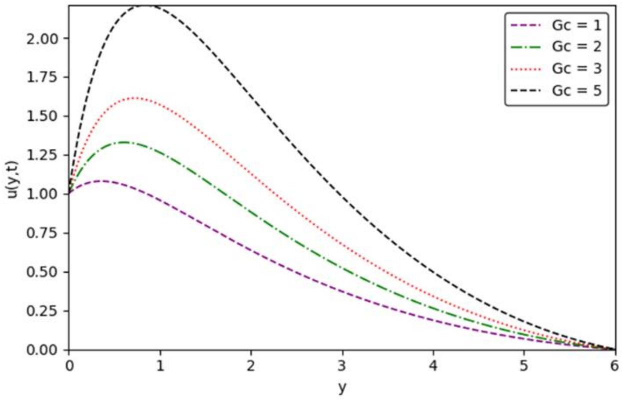

Figure 13. *Effect of mass Grashof number on the velocity profile.*

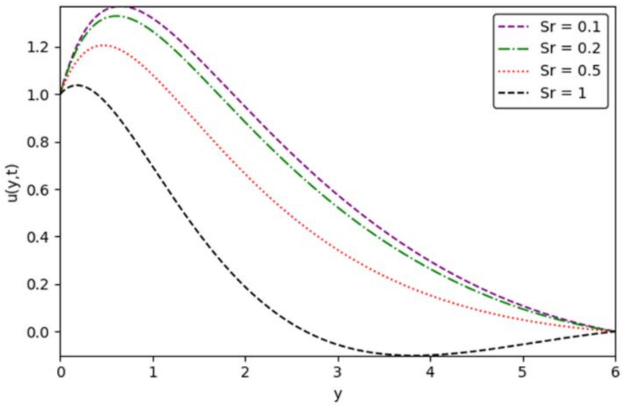

Figure 14. *Effect of Soret parameter on the velocity profile.*

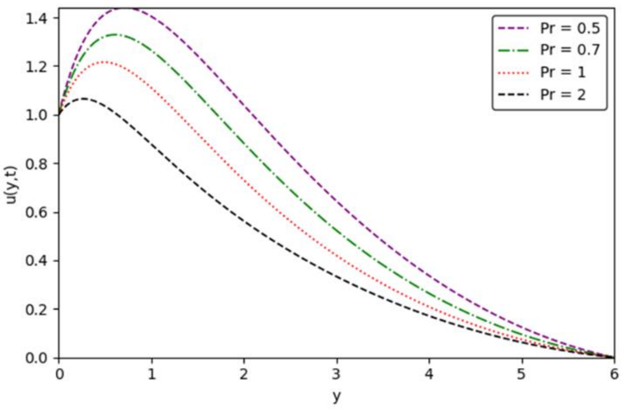

Figure 15. *Effect of Prandtl number on the velocity profile.*

Figure 1 presents the effect of the magnetic parameter on the velocity profile. It is observed that increasing the magnetic parameter significantly suppresses the fluid velocity. This behaviour is attributed to the Lorentz force generated by the applied magnetic field, which acts opposite to the direction of fluid motion, thereby increasing the resistive force and reducing the momentum boundary layer thickness.

The influence of the porosity parameter on the velocity profile is depicted in Figure 2. The results indicate that increasing the porosity parameter decreases the fluid velocity. Physically, a less permeable porous medium offers greater resistance to fluid motion, thereby weakening the flow and reducing the velocity boundary layer.

Figure 3 illustrates the effect of the solutal Grashof number on the velocity distribution. The velocity profile increases with increasing values of the solutal Grashof number. This enhancement is due to the stronger buoyancy force arising from concentration differences, which accelerates the fluid and thickens the momentum boundary layer.

The variation of the temperature profile with the Prandtl number is shown in Figure 4. The temperature decreases as the Prandtl number increases. This behaviour is expected because fluids with higher Prandtl numbers possess lower thermal diffusivity, which restricts heat diffusion within the boundary layer and consequently reduces the thermal boundary layer thickness.

Figure 5 demonstrates the influence of the heat generation parameter on the temperature profile. It is observed that increasing the heat generation parameter enhances the temperature distribution throughout the boundary layer. This is because internal heat generation supplies additional thermal energy to the fluid, resulting in an elevated temperature field.

The effect of the Soret parameter on the temperature profile is presented in Figure 6. The results reveal that increasing the Soret parameter reduces the temperature distribution. The thermo-diffusion mechanism facilitates species migration induced by temperature gradients, thereby redistributing thermal energy and leading to a reduction in the thermal boundary layer.

Figure 7 illustrates the influence of the Schmidt number on the temperature profile. The results show that the temperature profile increases with increasing Schmidt number. This behaviour suggests that reduced mass diffusivity modifies the thermal transport process, leading to a slight enhancement of the temperature field within the boundary layer.

Figure 8 depicts the effect of the Prandtl number on the concentration profile. It is observed that increasing the Prandtl number decreases the concentration distribution. The reduction in thermal diffusivity associated with larger Prandtl numbers weakens the coupled heat and mass transfer process, resulting in a thinner concentration boundary layer.

The influence of the Dufour number on the concentration profile is displayed in Figure 9. The results indicate that increasing the Dufour number enhances the concentration profile. This enhancement arises from the diffusion-thermo effect, whereby concentration gradients contribute to heat transport, thereby strengthening the coupled mass transfer process.

Figure 10 shows the effect of the heat generation parameter on the concentration profile. The concentration profile increases with increasing heat generation. The additional thermal energy supplied to the fluid promotes species transport, leading to an increase in concentration within the boundary layer.

Figure 11 illustrates the influence of the Soret parameter on the concentration profile. It is observed that the concentration profile decreases as the Soret parameter increases, indicating an inverse relationship. The enhanced thermo-diffusion effect redistributes the species concentration, thereby reducing the thickness of the concentration boundary layer.

Figure 12 presents the effect of the mass Grashof number on the temperature profile. The results demonstrate that increasing the mass Grashof number enhances the temperature distribution. The stronger concentration-induced buoyancy force intensifies convective transport, thereby increasing the thermal energy within the boundary layer.

Figure 13 illustrates the influence of the mass Grashof number on the velocity profile. An increase in the mass Grashof number significantly enhances the fluid velocity due to the increased buoyancy force generated by concentration gradients, which accelerates the flow.

Finally, Figures 14 and 15 show the effects of the Soret parameter and the Prandtl number on the velocity profile, respectively. In both cases, the velocity profile decreases with increasing parameter values. While the Soret parameter weakens the momentum transport through thermo-diffusion effects, higher Prandtl numbers reduce thermal diffusion, thereby diminishing buoyancy-driven acceleration and suppressing the fluid velocity.

7. Conclusion

The effect of thermal-diffusion on Magnetohydrodynamic Flow of an unsteady Chemically Reactive Fluid Passing through an Inclined Porous Plate Embedded in a Porous Medium is investigated in this study. The governing dimensional transient partial differential equations are transformed into dimensionless form using appropriate dimensional variables. Parametric study on the physical parameters such as porosity parameter, Magnetic field parameter, Soret effect, Dufour effect, solutal Grashof number, Mass Grashof number, angle of inclination, Schmidt number, Prandtl number, heat source/sink, chemical reaction, and thermal radiation on the flow distributions showed a profound impact. The key findings of the study are itemized as follows:

1) Increasing the magnetic parameter (M) suppresses the fluid velocity due to the Lorentz force, which opposes fluid motion and reduces the momentum boundary layer thickness.
2) An increase in the porosity parameter (K) decreases the velocity profile, indicating that greater porous medium resistance weakens the flow.
3) Higher values of the mass (solutal) Grashof number (Gc) enhance both the velocity and temperature profiles by strengthening concentration-induced buoyancy forces.
4) Increasing the Prandtl number (Pr) reduces the temperature, concentration, and velocity profiles, owing to the reduction in thermal diffusivity and the associated weakening of buoyancy-driven transport.
5) The heat generation parameter (Q) significantly increases both the temperature and concentration distributions by supplying additional thermal energy to the fluid.
6) An increase in the Soret parameter (Sr) suppresses the temperature, concentration, and velocity profiles,

demonstrating the influence of thermo-diffusion on coupled transport processes.

7) Increasing the Schmidt number (Sc) slightly enhances the temperature profile, indicating that reduced mass diffusivity modifies the coupled heat and mass transfer mechanism.
8) The Dufour number (Du) enhances the concentration profile, confirming the important role of diffusion-thermo effects in coupled heat and mass transfer within the porous medium.

Abbreviations

MHD	Magnetohydrodynamics
RDTM	Reduced Differential Transform Method
TAM	Temimi-Ansari Method
ADM	Adomian Decomposition Method

Author Contributions

Henry Martyns: Conceptualization, Formal Analysis, Investigation, Methodology

Liberty Ebiwareme: Validation, Visualization, Writing – original draft

Roseline Ize Ndu: Writing – review & editing

Conflicts of Interest

The authors declare no conflicts of interest.

Appendix

$$m_1=\frac{S+\sqrt{S^2-4\left(\frac{1+R}{Pr}\right)Q}}{2\left(\frac{1+R}{Pr}\right)}, m_2=\frac{ScS+\sqrt{S^2Sc^2+4K_rSc}}{2}, m_3=\frac{S+\sqrt{S^2+4(M+K)}}{2}$$

$$m_4=\frac{S+\sqrt{S^2-4\left(\frac{1+R}{Pr}\right)(Q-n)}}{2\left(\frac{1+R}{Pr}\right)}, m_5=\frac{ScS+\sqrt{S^2Sc^2+4Sc(K_r+n)}}{2}, m_6=\frac{S+\sqrt{S^2+4(M+K+n)}}{2}$$

$$A=-\frac{Sr\,m_1^2}{\frac{m_1^2}{Sc}-Sm_1-K_r}, B=-\frac{\cos\alpha(Gr+GcA)}{m_1^2-Sm_1-(M+K)}, C=-\frac{Gc(1-A)\cos\alpha}{m_2^2-Sm_2-(M+K)}$$

$$D=-\frac{Sr\,m_4^2}{\frac{m_4^2}{Sc}-Sm_4-(K_r+n)}, E=-\frac{\cos\alpha(Gr+GcD)}{m_4^2-Sm_4-(M+K+n)}, F=-\frac{Gc(1-D)\cos\alpha}{m_5^2-Sm_5-(M+K+n)}$$

$$C_1=1-A, C_2=1-B-C, D_1=1-D, E_1=1-E-F,$$

References

[1] Mopuri, O., Kodi, R., Madhu, M. R., Peram, C. G., Lorenzini, G., & Sidik, N. A. (2022). Unsteady MHD on convective flow of a Newtonian fluid past an inclined plate in presence of chemical reaction with radiation absorption and Dufour effects. CFD Letters, 14(7), 62–76. https://doi.org/10.37934/cfdl.14.7.6276

[2] Nayak, A., & Rath, C. (2023). Visco-elastic impacts on an unsteady MHD flow past a constant slanted plate in the presence of viscous dissipation, radiation and chemically reactive species: A numerical study. Journal of Naval Architecture and Marine Engineering. https://doi.org/10.3329/jname.v20i2.61193

[3] Krishna, M. V., Ahamad, N. A., Ahamad, A., & Chamkha, A. J. (2020). Hall and ion slip effects on unsteady MHD free convective rotating flow through a saturated porous medium over an exponentially accelerated plate. Alexandria Engineering Journal, 59(2), 565–577. https://doi.org/10.1016/j.aej.2020.01.043

[4] Malapati, V., & Makinde, O. D. (2018). Unsteady MHD slip flow with radiative heat and mass transfer over an inclined plate embedded in a porous medium. Defect and Diffusion Forum, 384, 31–48. https://doi.org/10.4028/www.scientific.net/DDF.384.31

[5] Ali, F., Khan, I., & Shafie, S. (2013). Conjugate effects of heat and mass transfer on MHD free convection flow over an inclined plate embedded in a porous medium. PLOS ONE, 8(6), e65223. https://doi.org/10.1371/journal.pone.0065223

[6] Rani, K. J., Reddy, G. V. R., & Murthy, M. V. R. (2016). Heat and mass transfer effects on MHD free convection flow over an inclined plate embedded in a porous medium. International Journal of Chemical Sciences, 13(4), 1998–2016.

[7] Seth, G. S., Tripathi, R., Sharma, R., & Chamkha, A. J. (2017). MHD double diffusive natural convection flow over an exponentially accelerated inclined plate. Journal of Mechanics. https://doi.org/10.1017/jmech.2016.56

[8] Endalew, M. F., & Sarkar, S. (2021). Incidences of aligned magnetic field on unsteady MHD flow past a parabolic accelerated inclined plate in a porous medium. Heat Transfer. https://doi.org/10.1002/htj.22153

[9] Rani, B. R. (2018). Effects of radiation and Hall current on unsteady MHD free convective flow over inclined porous surface. International Journal of Mechanical and Production Engineering Research and Development, 8(4), 1177–1186. https://doi.org/10.24247/ijmperdaug2018121

[10] Basha, P. M. S., & Nagarathna, N. (2019). Heat and mass transport on MHD free convective flow through a porous medium past an infinite vertical plate. International Journal of Applied Engineering Research, 14(21), 4067–4076.

[11] Malga, B. S., & Kishan, N. (2014). Finite element analysis for unsteady MHD heat and mass transfer free convection flow of polar fluids past a vertical moving porous plate in a porous medium with heat generation and thermal diffusion. Journal of Naval Architecture and Marine Engineering, 11(1), 69–82. https://doi.org/10.3329/jname.v11i1.12844

[12] Reddy, B. P. (2017). Thermal diffusion and Hall effects on MHD flow past an impulsively started inclined plate with variable temperature and mass diffusion in the presence of thermal radiation. International Journal of Engineering Research and Applications, 7(7), 55–66. https://doi.org/10.9790/9622-0707055566

[13] Saidulu, B. (2018). Role of magnetic field on natural convection towards a semi-infinite vertically inclined plate in the presence of Hall current with numerical solutions: A finite difference technique. International Journal of Mathematics Trends and Technology, 6(2), 25–40.

[14] Jayakar, R., Kumar, B. R., & Makinde, O. D. (2018). Thermo diffusion effects on MHD chemically reacting fluid flow past an inclined porous plate in a slip flow regime. Defect and Diffusion Forum, 387, 587–599. https://doi.org/10.4028/www.scientific.net/DDF.387.587

[15] Reddy, B. P., Simba, M., & Hugo, A. (2023). Effects of thermodiffusion and chemical reaction on magnetohydrodynamic-radiated unsteady flow past an exponentially accelerated inclined permeable plate embedded in a porous medium. International Journal of Chemical Engineering, 2023, Article 9342174. https://doi.org/10.1155/2023/9342174

[16] Shaik, H., Bommireddy, V. K. R., Lam, S., & Palaparthi, K. K. (2023). Radiation absorption and diffusion thermo effects on unsteady MHD Kuvshinski fluid flow past an inclined porous plate in the presence of thermal radiation and chemical reaction. Journal of Advanced Research in Fluid Mechanics and Thermal Sciences, 109(1), 162–176. https://doi.org/10.37934/arfmts.109.1.162176

[17] Mopuri, O., Sailakumari, A., Ganjikunta, A., Sudhakara, E., Venkateswara Raju, K., Ramesh, P., Ganteda, C., Ramakrishna Reddy, B., & Varma, S. V. K. (2024). Characteristics of MHD Jeffery fluid past an inclined vertical porous plate. CFD Letters, 16(6), 68–89. https://doi.org/10.37934/cfdl.16.6.6889

[18] Ebiwareme, L., Bunonyo, K. W., & Davies, O. A. (2023). Heat transfer analysis of magnetohydrodynamics fluid flow past an infinite vertical porous plate in the presence of suction: The Adomian decomposition approach. American Journal of Engineering Research, 12(2), 146–160.

[19] Ebiwareme, L., Bunonyo, K. W., & Tasie, N. N. (2023). Analytical investigation of MHD Casson fluid flow past an inclined semi-infinite porous plate with radiation absorption and magnetic field effects. International Research Journal of Innovations in Engineering and Technology, 7(4), 45–55. https://doi.org/10.47001/IRJIET/2023.704007

[20] Ebiwareme, L., & Bunonyo, K. W. (2023a). Application of approximation technique for the effects of chemical reaction and radiation absorption of MHD fluid flowing past an inclined porous plate in the presence of inclined magnetic field. International Journal of Advances in Applied Mathematics and Mechanics, 11(1), 30–41.

[21] Ebiwareme, L., & Bunonyo, K. W. (2023b). MHD fluid flowing through a vertical porous plate with the influence of a magnetic field and an angle of inclination using the method of reduced differential transformation. Asian Journal of Pure and Applied Mathematics, 5(1), 179–193.